Available online at www.sciencedirect.com

SciVerse ScienceDirect

Ceramics International 38 (2012) 5411–5418

CERAMICS INTERNATIONAL

www.elsevier.com/locate/ceramint

Aqueous gelcasting of ZrB_2–SiC ultra high temperature ceramics

Rujie He *, Xinghong Zhang, Ping Hu, Chen Liu, Wenbo Han

National Key Laboratory of Science and Technology on Advanced Composites in Special Environments, Harbin Institute of Technology, Harbin 150001, PR China

Received 8 January 2012; received in revised form 24 February 2012; accepted 21 March 2012
Available online 29 March 2012

Abstract

ZrB_2–SiC ultra high temperature ceramics containing B_4C and C as sintering additives were successfully prepared by aqueous gelcasting and pressureless sintering. Polyacrylic acid (PAA) was used as the dispersant throughout this research. The various effects of zeta potential, pH value, dispersant concentration, solid loading and ball-milling time on the rheology and fluidity behavior of ZrB_2–SiC suspension were investigated in detail. A well-dispersed suspension with 50 vol.% solid loading was prepared at pH 10 with 0.4 wt.% PAA after ball milling at 240 rpm for 24 h. Then crack-free green ZrB_2–SiC ceramics were obtained by gelcasting process and then pressureless sintered at 2100 °C to about 98% relative density. The microstructure and mechanical properties were examined, and the flexural strength and fracture toughness were 405 ± 27 MPa and 4.3 ± 0.3 MPa $m^{1/2}$, respectively.

Keywords: B. Microstructure-final; C. Mechanical properties; D. Borides; Aqueous gelcasting

1. Introduction

Zirconium diboride (ZrB_2), known as ultra high temperature ceramic (UHTC), has unique combination properties such as ultra high melting point, high electrical and thermal conductivities, high hardness, good chemical inertness, as well as high wear resistance [1–3]. All of those excellent properties make ZrB_2 the most promising candidate for ultra high temperature applications, such as sharp leading edges and nosecones, and thermal protection systems for reusable atmosphere re-entry vehicles, hypersonic flight, and rocket propulsion systems [4–6].

Because of its strong covalent bonding and low self-diffusion coefficient, monolithic ZrB_2 is always added by SiC particles to promote the densification, mechanical properties and oxidation resistance [7]. As a rule, the hot pressing (HP) technique is conducted at temperature above 1800 °C, depending on the sintering parameters (pressure, soaking time, heating rate) and/or sintering additives [8]. However, the HP process is usually limited to the formation of relatively simple geometrical and moderate sizes. Fabrication of components with complex shapes requires costly and time-consuming electrical discharge machining from a hot-pressed billet. Recently, a number of pressureless sintering routes have been developed for ZrB_2-based ceramics [9–12]. These breakthroughs have provided great opportunities for achieving the densification of ZrB_2-based ceramics through conventional powder processing routes, including colloidal processing. In order to obtain near-net and complex-shaped green bodies of ZrB_2-based ceramics, a number of colloidal methods have been used, i.e., slip casting [13,14], tape casting [15–17], and freeze-form extrusion fabrication [18].

Gelcasting is an attractive forming process for achieving high-quality, complex-shaped ceramic parts [19]. This process is a colloidal-forming process, based on in situ solidification of the ceramic slurry by the polymerization of monomers. In this process, the ceramic powder is dispersed into a monomer solution and then, after adding catalyst and initiator, it is poured into a mold, polymerized in situ to immobilize the particles in the gelled part, then removed from the mold while still wet, and finally dried and sintered in a conventional way. Gelcasting technique has widely been used to prepare all kinds of ceramics, including oxides [20,21] and non-oxides [22,23]. Up to now, however, the availability of literature on gelcasting technique of UHTCs is quite scarce.

In this study, the dispersion, stability, rheology and fluidity behavior of ZrB_2–SiC aqueous suspension were investigated in detail, and crack-free green ZrB_2–SiC ceramics (containing

* Corresponding author. Tel.: +86 451 86403016; fax: +86 451 86403016.
E-mail address: herujie2003jci@163.com (R. He).

0272-8842/$36.00
http://dx.doi.org/10.1016/j.ceramint.2012.03.051

B_4C and C as sintering additives) were obtained by gelcasting and then pressureless sintered at 2100 °C for 2 h. Microstructure and mechanical properties were also characterized and discussed.

2. Materials and methods

2.1. Raw materials

Commercial ZrB_2 powder (2 μm; purity > 99.5%; Northwest Institute for Non-ferrous Metal Research, Xi'an, China) and SiC powder (0.5 μm; purity > 99%; Weifang Kaihua Micro-powder Co. Ltd., Weifang, China) were used as raw materials in the present work. B_4C powder (0.5 μm; purity > 98%; Jingangzuan Boron Carbide Co. Ltd., Mudanjiang, China) and carbon black powder (0.5 μm; purity > 99%; Qingdao Tiansheng Graphite Co. Ltd., Qingdao, China) were used as sintering additives. The mixture of ZrB_2–20 vol.% SiC–2 vol.% B_4C–2 vol.% C was ball-milled in ethanol for 8 h with zirconia media in a planetary mill (MCA-10B, Nanjing University Instrument Plant, Nanjing, China) at 240 rpm (revolutions per minute). After milling, ethanol was removed through a rotating evaporator (R-202, Shanghai Shensheng Biotech Co. Ltd., Shanghai, China) at 70 °C to minimize segregation and then sieved through a 200 mesh. The morphology of as-received ZrB_2–SiC–B_4C–C mixed powder is shown in Fig. 1.

2.2. Aqueous gelcasting and pressureless sintering procedure

Aqueous gelcasting was carried out by using acrylamide [$C_2H_3CONH_2$] (AM) as monomer and *N*,*N*′-methylenebisacrylamide [$(C_2H_3CONH)_2CH_2$] (MBAM) as coupling agent. Initiator of polymerization was ammonium persulphate [$(NH_4)_2S_2O_8$] (APS). The catalyst was *N*,*N*,*N*′,*N*′-tetramethylethylenediamine [$C_6H_{16}N_2$] (TEMED). Dispersant used for suspension stabilization was polyacrylic acid (PAA,

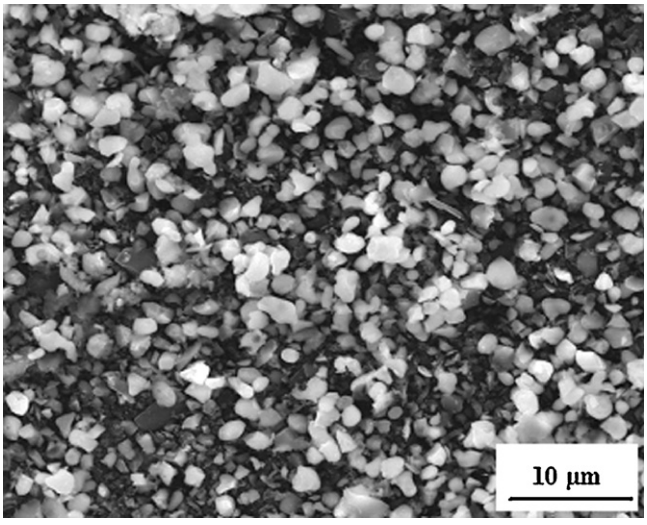

Fig. 1. SEM of ZrB_2–SiC powder containing B_4C and C as sintering additives.

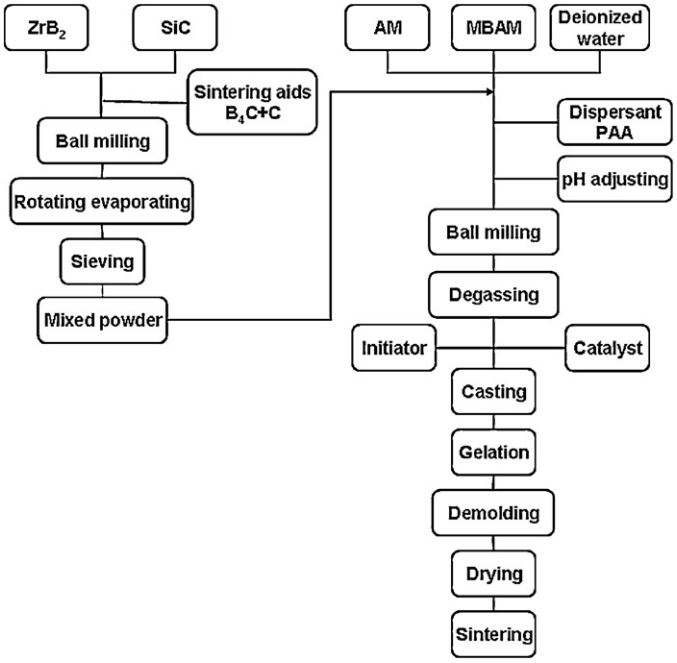

Fig. 2. Flow chart of the gelcasting process.

M_w = 3000). Fig. 2 illustrates the flow chart of the gelcasting process. First, the monomer (AM) and the coupling agent (MBAM) were dissolved in deionized water to form a solution (deionized water:AM:MBAM = 20:1:0.05). After adding ZrB_2–SiC–B_4C–C mixed powder, PAA with different concentrations (0–1.0 wt.%, based on mixed powder) were added to the solution. The suspension pH was adjusted from 2 to 13 by hydrochloric acid (HCl) and ammonia water (NH_4OH). In order to break down agglomerates, the suspension was ball milled at 240 rpm for different time (10 min to 30 h). Degassing was subsequently carried out for 10 min in a rotating vacuum equipment (TP-08, Beijing Orient Sun-Tec Co. Ltd., Beijing, China). Both of the initiator (APS) and catalyst (TEMED) were then subsequently added to the suspension. Then the resulting suspension was finally poured into a nonporous plastic mold. After the monomers polymerized, the gelled wet body was demolded after 6 h and dried at room temperature for 48 h. After drying, binder burnout and pressureless sintering were accomplished in a high temperature graphite resistant furnace (ZRY-80, Jinzhou Hangxing Vacuum Equipment Co. Ltd., Jinzhou, China). The whole sintering schedule included external isothermal holds at 600 °C and 1600 °C for 30 min in vacuum (15 Pa), respectively, and then argon gas (1 atm) was then introduced into the furnace. The gelcast ceramic was then continually pressureless sintered to 2100 °C with a holding time of 2 h.

2.3. Measurements

Zeta potential measurements of single ZrB_2 and SiC with or without 0.5 wt.% PAA as dispersant were conducted separately as a function of pH value (in the range of 2–13) via Zeta potential analyzer (Zetasizer Nano ZS, Malvern, UK).

Rheological behavior of the suspension was determined using a rotational viscometer (NDJ-1B, Shanghai Pingxuan Instrument Co. Ltd., Shanghai, China). Fluidity behavior of the suspension was measured by counting the time in seconds for the running of 100 ml suspension out of a specified container. Binder burnout behavior of the green body was determined using thermo gravimetric and differential thermal analysis (TG–DTA, Netzsch STA 449C, Germany) in nitrogen at a heating rate of 10 °C/min up to 900 °C. Commercial software package (HSC Chemistry 5.11, Outkumpu Research Oy, Finland) was used to perform the thermodynamic calculations. The bulk density of the green gelcasting body and as-sintered sample was measured by Archimedes' method in deionized water, and the theoretical density was calculated by applying the law of mixture. Microstructure of the polished surface was analyzed using scanning electron microscopy (SEM, FEI Sirion 200, Philips, Holland). Commercial software package (Image Pro-plus 6.0, Media Cybernetics, USA) was applied to measure the grain size on an average of 100 grains. Flexural strength (σ) was measured by using three-point bending tests (Model 3369, Instron, USA) on 36 mm × 4 mm × 3 mm (length × width × thickness) test bars, using a loading span of 30 mm with a crosshead speed of 0.5 mm/min at room temperature. Fracture toughness (K_{IC}) was evaluated using single-edge notched bend (SENB) beams 22 mm × 4 mm × 2 mm (length × height × width), with a notched depth and width of 2 and 0.2 mm, respectively, using a span of 16 mm and a crosshead speed of 0.05 mm/min.

3. Results and discussion

3.1. Zeta potential measurements

Fig. 3 shows the zeta potentials of single ZrB_2 and SiC suspension with and without 0.5 wt.% PAA as dispersant at different suspension pH. The zeta potentials of the sintering additives, B_4C and C, were not taken into account due to their small content in the suspension. According to the measurement, the isoelectric point (IEP, the pH at which the net charge on the particle surface is zero) for ZrB_2 and SiC was pH 6.7 and pH 4.2, respectively. In the vicinity of the IEP, the particles had low zeta potentials which may either positive ($pH < pH_{iep}$) or negative ($pH > pH_{iep}$), so suspensions prepared within this pH region got highly flocculated by van der Waals forces of attraction between the particles due to the absence of repulsive forces, resulting in colloidal unstable suspensions consist of large agglomerates that were likely to lead to flaw during gelcasting. When adding 0.5 wt.% PAA, the IEP for ZrB_2 and SiC was decreased from pH 6.7 to pH 5.8 and from pH 4.2 to pH 3.5, respectively. Besides, it was clearly observed that both ZrB_2 and SiC particles doped with PAA had high negative zeta potentials at pH 10–12, indicating that both ZrB_2 and SiC powders could be well dispersed in this pH range. The zeta potentials of ZrB_2–SiC–B_4C–C mixture with and without PAA are also exhibited in Fig. 3. Similar characters were also observed for mixed suspension. The dispersion of mixed suspension could be obtained in the pH range of 10–12.

3.2. Rheological property and fluidity behavior of suspension

3.2.1. Effects of dispersant concentration on the suspension rheology and fluidity

The effects of dispersant concentration on the viscosity and fluidity of ZrB_2–SiC suspensions with 20 vol.% solid loading at pH 10 are given in Fig. 4. The lowest viscosity was obtained at the PAA concentration of 0.4 wt.%, which indicated a well dispersed suspension was obtained. On one hand, when PAA concentrations below 0.4 wt.%, the increase of the viscosity was attributed to unsaturated adsorption of the dispersant, inducing low electrostatic repulsion between particles and thereby forcing particles together. On the other hand, when PAA concentrations above 0.4 wt.%, over-saturated adsorption of PAA not only increased the ionic strength of the solution and compressed the double layer, resulting in the electrostatic repulsion decrease between particles, but also increased the bridging flocculation because of polyelectrolyte macromole-

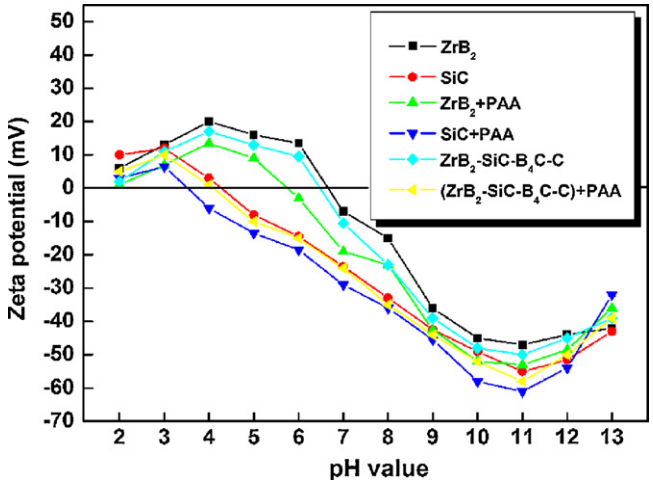

Fig. 3. Zeta potentials of ZrB_2, SiC and ZrB_2-SiC-B_4C-C mixture with or without 0.5 wt.% PAA as dispersant.

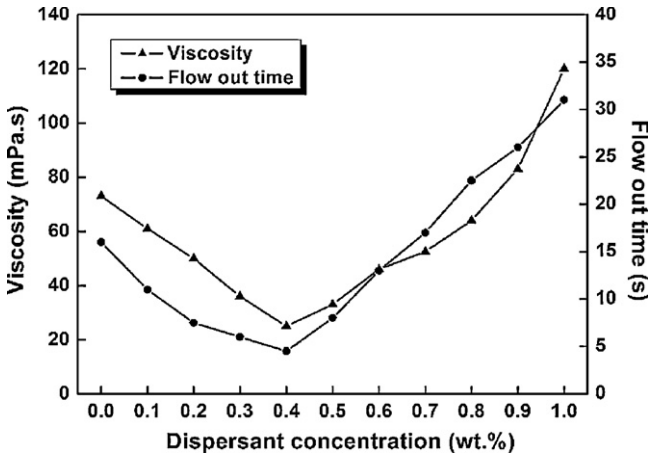

Fig. 4. Effect of dispersant (PAA) concentration on the viscosity (shear rate, 60 s^{-1}) and fluidity of ZrB_2–SiC suspensions (20 vol.% solid loading, pH = 10, 240 rpm for 24 h).

cule. Both of unsaturated adsorption and over-saturated adsorption were harmful to the particle dispersing in the solvent, and thus the viscosity of the suspension had an inevitable increase. Moreover, it was also found that the flow out time of the ZrB_2–SiC suspension reduced to about 4 s when 0.4 wt.% dispersant was added. Hence, when adding 0.4 wt.% dispersant, the state of dispersant on the particle surface was saturated adsorption, finally obtaining a low viscosity ZrB_2–SiC suspension.

3.2.2. *Effects of pH value on the suspension rheology and fluidity*

The effects of pH value on the rheology and fluidity of ZrB_2–SiC suspensions with 0.4 wt.% PAA were further investigated, as shown in Fig. 5. At pH 9–11, the suspension was more stable and the viscosity was much lower, which were in good accordance with the zeta potential measurements (as shown in Fig. 3). In particular, the ZrB_2–SiC suspension had the lowest viscosity at pH 10. Due to the change of pH not only influenced the zeta potential of particles but also influenced the ionization degree and adsorption configuration of polymer. The increase in pH values led to the increase of the negative charge of particle surface and PAA adsorption on it was almost entirely ionized at pH 10, finally causing enlarging zeta potential and enhancing electrostatic repulsion. At the same time, the tails and loops configurations of the polymer (PAA) were so dominant that the steric repulsion was also the strongest at pH 10. When the pH value further increased, the adsorption amount of PAA reduced and the remains of PAA in solution increased the viscosity. Besides, with the further increase in pH value, the ion concentration increased, which resulted in the compressing of double layer and the reducing of zeta potential (as shown in Fig. 3). When the pH of ZrB_2–SiC suspension was 10, the flow out time was less than 5 s. Therefore, the optimum pH value was chosen as pH 10.

3.2.3. *Effects of solid loading on the suspension rheology and fluidity*

Fig. 6(a) shows the rheological behavior of ZrB_2–SiC suspensions vs. different solid loading. It could be observed that the ZrB_2–SiC suspensions with 20, 30, 40 and 50 vol.% solid loading exhibited obviously so-called "shear-thinning" behavior in rheology. It was well known that colloidal stable suspension exhibited shear-thinning behavior due to the perturbation of the suspension structure by shear. The suspension microstructure was equilibrium because thermal motion dominated over the viscous forces at low shear rates. However, the suspension microstructure was affected by the viscous forces, and shear-thinning happened at high shear rates. At very high shear rates, the viscous forces dominated and the plateau of viscosity indicated the resistance to flow of the suspension with a completely hydrodynamically controlled microstructure. Obviously, the degree of shear-thinning and the viscosity at high shear rates increased with the solid loading increasing. The fluidity decreased with the increase in solid loading because of the coagulation of particles (as shown in Fig. 6(b)). The ZrB_2–SiC suspension with 50 vol.% solid loading still had a relative low viscosity of 3.1 Pa s at the shear rate of 60 s^{-1} and flow out time of less than 5 s, which met the demands of aqueous gelcasting process. Considering higher solid loading would be benefit to the gelcasting and sintering

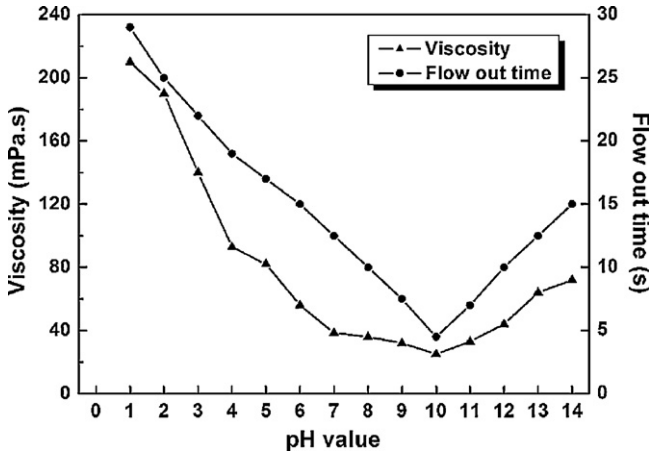

Fig. 5. Effect of pH value on the viscosity (shear rate, 60 s^{-1}) and fluidity of ZrB_2–SiC suspensions (20 vol.% solid loading, 0.4 wt.% PAA, 240 rpm for 24 h).

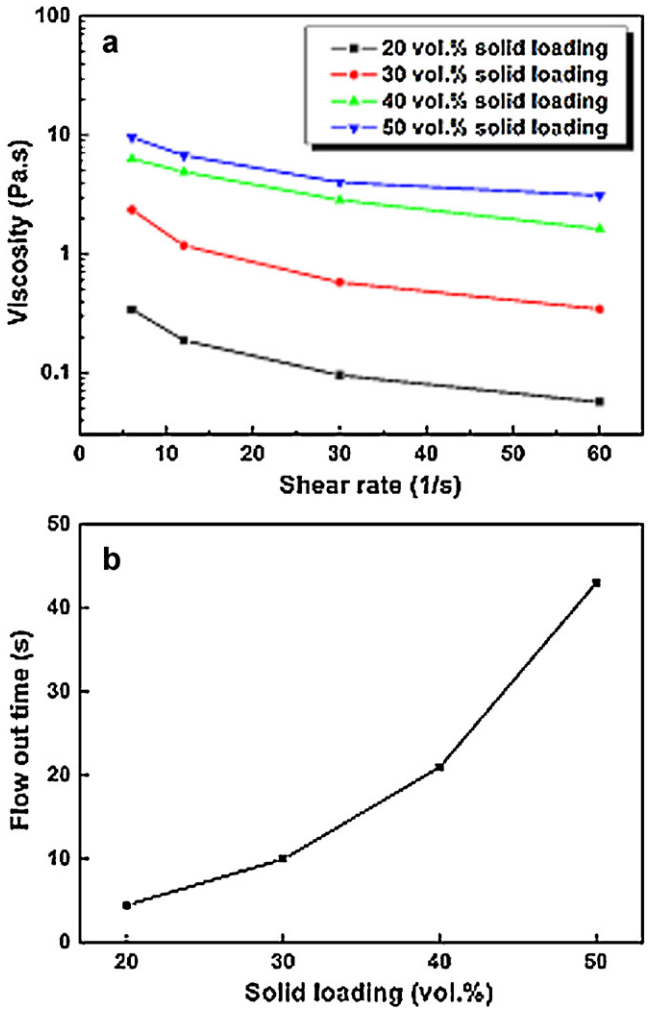

Fig. 6. Effect of solid loading on the viscosity and fluidity of ZrB_2–SiC suspensions (pH 10, 0.4 wt.% PAA, 240 rpm for 24 h): (a) viscosity vs. solid loading at different shear rates; (b) flow out time vs. solid loading.

process, the solid loading of the ZrB_2–SiC suspension was chosen as 50 vol.%.

3.2.4. Effects of ball milling time on the suspension rheology and fluidity

The typical effects of ball milling time (10 min to 30 h) on the apparent viscosity and fluidity behavior of ZrB_2–SiC suspension with 50 vol.% solid loading are given in Fig. 7. When the ball milling time was shorter than 20 h, the viscosity of the suspension decreased and the fluidity increased gradually as the time of ball milling increased. The reason was that the adsorption of dispersant on particle surface did not reach equilibrium and the suspension was not colloidal stable. However, the apparent viscosity and fluidity of the ZrB_2–SiC suspension were consistent after 20 h milling, because the PAA dispersant had been totally adsorbed on particle surface. Therefore, the ball milling time should be set as equal to or more than 20 h in order to obtain a well dispersed suspension.

3.3. Aqueous gelcasting, binder burnout and sintering

In the present research, the PAA concentration and the pH value was set as 0.4 wt.% and pH 10, respectively. The ZrB_2–SiC suspension (containing B_4C and C) with 50 vol.% solid loading was ball milled at 240 rpm for 24 h. Then the gelcasting process was conducted. After drying, crack-free green body was obtained. The green density and green strength of the dried green body could reach to about 48% of the theoretical density and 45 MPa, respectively. Before sintering, the organic additives incorporated into the green bodies during gelcasting fabrication should be removed. One of the advantages of gelcasting was the small amount of polymer that remained in the green bodies after drying. The dried body contained only about 5 wt.% polymer. TG/DTA analysis of the dried green body was carried out under the N_2 protection from room temperature to 900 °C, as shown in Fig. 8. An approximately 1 wt.% reduction in dried body at about 120 °C was observed due to the vaporization of the residual water in the green body.

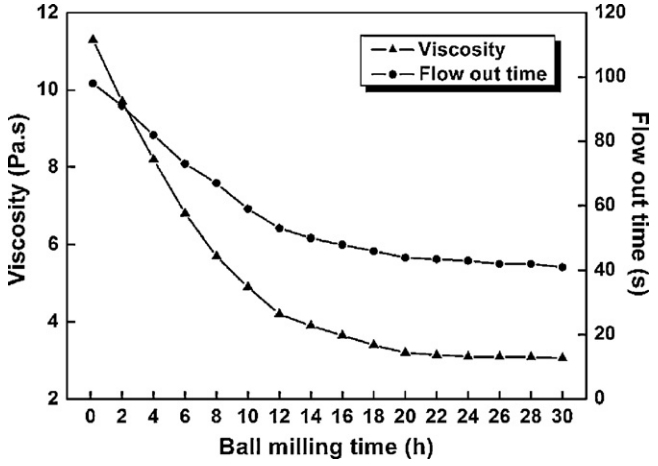

Fig. 7. Effect of ball milling time on the viscosity and fluidity of ZrB_2–SiC suspensions (pH, 10; PAA concentration, 0.4 wt.%; shear rate, 60 s^{-1}; ball milling speed, 240 rpm).

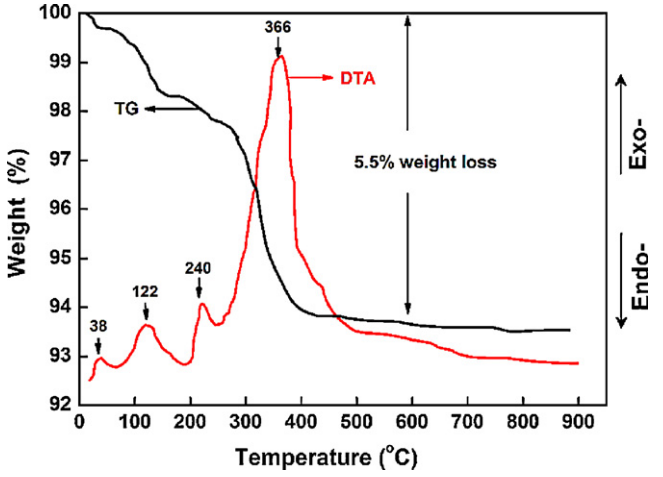

Fig. 8. TG/DTA analysis for the dried green body in N_2.

The vaporization of the residual water caused obvious exothermic DTA peaks at 38 °C and 122 °C. Furthermore, the organic additives were burnt at temperatures ranging from 200 to 450 °C, resulting in an obvious exothermic DTA peak and a weight loss TG peak. The exothermic peaks at 240 °C and 366 °C were mainly resulting from the pyrolysis of dispersant (PAA) and polyacrylamide in the gel. The residual water could be fully vaporized and the organic binder could be finally burnout, owing to about 5.5 wt.% loss occurring at temperatures up to 600 °C. Therefore, the dried green body was firstly heated up to 600 °C at a heating rate of 1 °C/min in order to remove the residual water and binders.

For ZrB_2, the surface oxide impurities (such as B_2O_3 and ZrO_2) played a critical role in sintering by promoting the evaporation–condensation mechanisms, which led to oxide-induced particle coarsening at temperatures below which densification of the underlying ceramic could proceed. As a result, particle coarsening caused the decrease of the driving force for densification and a limiting density, which was significantly below the desired level of 100% relative density. B_2O_3 could be removed by the evaporation at elevated temperatures, whereas ZrO_2 must be removed by chemical reactions. The literature reports [9–12] had showed that ZrB_2-based ceramics could pressureless sintered to about full density by using <4 wt.% boron carbide (B_4C) and/or carbon (C) as sintering additives, for the reason that B_4C and C could react with the surface oxide impurities and remove them, achieving finally densification at a relative low temperature. In our present research, the combination of B_4C and C was used as sintering additives to remove the surface oxide impurities. Therefore, the main expected reactions during sintering process are shown as follows,

$$7ZrO_2 + 5B_4C \rightarrow 7ZrB_2 + 3B_2O_3 + 5CO\,(g) \quad (1)$$

$$ZrO_2 + 5C + B_2O_3 \rightarrow ZrB_2 + 5CO\,(g) \quad (2)$$

$$2ZrO_2 + B_4C + 3C \rightarrow 2ZrB_2 + 4CO\,(g) \quad (3)$$

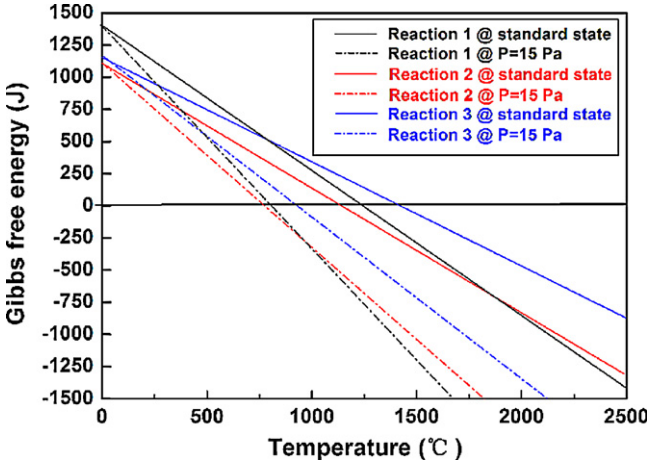

Fig. 9. Comparison of the Gibbs free energy as a function of temperature for Reactions (I)–(III) under standard state and $P = 15$ Pa.

Fig. 10. Morphology of UHTC configurations prepared by gelcasting and pressureless sintering of ZrB_2–SiC containing B_4C and C as sintering additives.

The Gibbs free energy calculations for Reactions (I)–(III) are given as follows [10],

$$\Delta G_T^\circ = 1378.7 - 0.9242T + RT \ln P_{co}^5 \quad \text{(I)}$$

$$\Delta G_T^\circ = 1099.6 - 0.7784T + RT \ln P_{co}^5 \quad \text{(II)}$$

$$\Delta G_T^\circ = 1134.1 - 0.6668T + RT \ln P_{co}^4 \quad \text{(III)}$$

The changes of Gibbs free energy for the reactions as a function of temperature under standard state ($P = 101.3$ kPa) and sintering condition ($P = 15$ Pa) have been plotted in Fig. 9. In standard state, each of these reactions became favorable ($\Delta G_T^\circ < 0$) at elevated temperatures. Specifically, Reactions (I), (II) and (III) were favorable above 1219, 1140, and 1428 °C, respectively. However, when P_{co} was 15 Pa, Reactions (I), (II) and (III) could occur at as low as 797, 775, and 911 °C, respectively. Therefore, when ZrB_2–SiC ceramics (containing B_4C and C) were sintered at 2100 °C with a holding at 1600 °C in vacuum ($P = 15$ Pa), Reaction (II) firstly occurred, then Reactions (I) and (III) occurred subsequently, which would react with the surface oxide impurities on ZrB_2 and remove them, finally achieving densification at a relative low temperature.

Fig. 10 demonstrates some examples of sintered UHTC configurations prepared by gelcasting and pressureless sintering of ZrB_2–SiC ceramic containing B_4C and C as sintering additives.

3.4. Microstructure and mechanical properties

For as-prepared ZrB_2–SiC ceramics, the additive of a combination of B_4C (2 vol.%) and carbon (2 vol.%) led to high relative density (>98%) at the sintering temperature as low as 2100 °C for 2 h. As shown in Fig. 11, the examination of the microstructure after sintering revealed an average grain size of about 5 μm for ZrB_2 grains and about 2 μm for SiC grains, and a very scarce residual porosity. The SiC particles, which represented the majority of the dark features, were homogeneously dispersed in the ZrB_2 matrix and no obvious agglomeration was detected. ZrO_2 and B_2O_3 were assumed as the main oxygen impurities on the surface of ZrB_2. Such a combination of B_4C and C as sintering additives could remove these surface oxide impurities by chemical reactions effectively

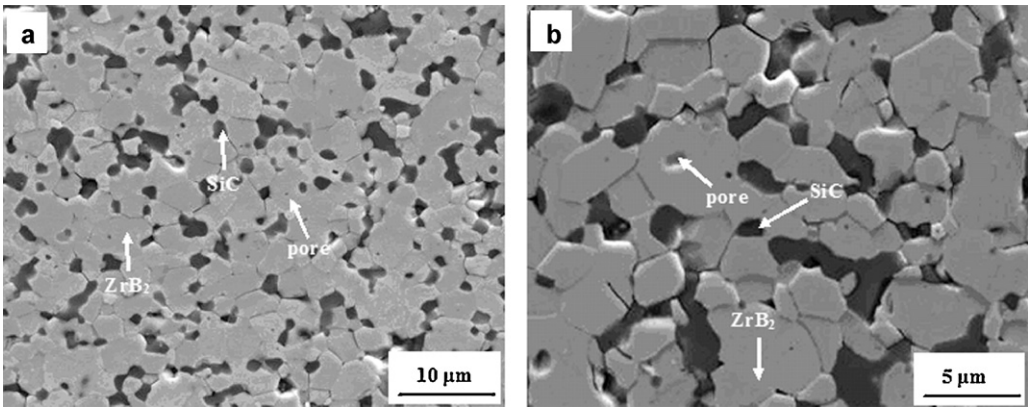

Fig. 11. SEM of the polished surface of the as-received ZrB_2–SiC ultra high temperature ceramics: (a) low magnification; (b) high magnification.

Table 1
Comparison of sintering conditions, density, and mechanical properties for hot pressed and gel casting-pressureless sintered ZrB_2–SiC ceramics.

ZrB_2–20SiC	Sintering additives	Sintering conditions	Rd (%)	σ (MPa)	K_{IC} (MPa $m^{1/2}$)
Hot pressing [24]	–	2000 °C, 30 MPa, 1 h	99.8	502 ± 45	4.25 ± 0.2
Gelcasting-pressureless sintering	$B_4C + C$	2100 °C, 2 h	~98	405 ± 27	4.3 ± 0.3

Rd, relative density; σ, flexural strength; K_{IC}, fracture toughness.

and thus promoted the densification. The flexural strength and fracture toughness for gelcasting-pressureless sintered ZrB_2–SiC ceramics were 405 ± 27 MPa and 4.3 ± 0.3 MPa $m^{1/2}$, respectively, which reached or exceeded the level of mechanical properties of hot pressed ZrB_2–SiC ceramics reported in our previous work [24]. The sintering conditions, relative density, and mechanical properties for hot pressed and gelcasting-pressureless sintered ZrB_2–SiC ceramics are listed in Table 1 for comparison. The 2% porosity existed in the as-prepared ceramics led to a low flexural strength. However, the pores in the ceramic would relax the stress and arrest the propagation of microcracks effectively, which resulted in a high fracture toughness.

4. Conclusions

In this present study, the dispersion, stability, rheological property and fluidity behavior of ZrB_2–20SiC suspensions (containing B_4C and C) for aqueous gelcasting were investigated in detail. ZrB_2–SiC ceramics were successfully prepared by aqueous gelcasting and pressureless sintering. Polyelectrolyte PAA was chosen as dispersant in this research. The various effects of zeta potential, pH value, dispersant concentration, solid loading and ball-milling time on the rheology and fluidity behavior of ZrB_2–SiC suspensions were studied systematically. A well-dispersed ZrB_2–SiC slurry with 50 vol.% solid loading was obtained at pH 10 with 0.4 wt.% PAA after ball milling at 240 rpm for 24 h. Then crack-free dried green ZrB_2–SiC ceramic samples were successfully fabricated by gelcasting process. The burnout of binder was conducted at 600 °C and the residual water and organic binders were removed. Then the samples were pressureless sintered at 2100 °C for 2 h (with a holding at 1600 °C to remove surface oxide impurities) to about 98% relative density. The average grain size was about 5 μm for ZrB_2 grains and about 2 μm for SiC grains. The SiC particles were homogeneously dispersed in the ZrB_2 matrix and no obvious agglomeration was detected. The flexural strength and fracture toughness were 405 ± 27 MPa and 4.3 ± 0.3 MPa $m^{1/2}$, respectively. This work can lay the foundation for the near-net shape forming and pressureless sintering of ZrB_2 based ultra high temperature ceramics.

Acknowledgment

This research was supported by ‘‘The Fundamental Research Funds for Central Universities’’ of China (Grant No. Hit. NSRIF. 2012030).

References

[1] F. Monteverde, A. Bellosi, S. Guicciardi, Processing and properties of zirconium diboride-based composites, J. Eur. Ceram. Soc. 22 (2002) 279–288.
[2] F. Monteverde, The thermal stability in air of hot-pressed diboride matrix composites for uses at ultra-high-temperatures, Corros. Sci. 47 (2005) 2020–2033.
[3] S.Q. Guo, T. Mizuguchi, M. Ikegami, Y. Kagawa, Oxidation behavior of ZrB_2–$MoSi_2$–SiC composites in air at 1500 °C, Ceram. Int. 37 (2011) 585–591.
[4] F. Monteverde, R. Savino, Stability of ultra-high-temperature ZrB_2–SiC ceramics under simulated atmospheric re-entry conditions, J. Eur. Ceram. Soc. 27 (2007) 4797–4805.
[5] S.R. Levine, E.J. Opila, M.C. Halbig, J.D. Kiser, M. Singh, J.A. Salem, Evaluation of ultra-high temperature ceramics for aeropropulsion use, J. Eur. Ceram. Soc. 22 (2002) 2757–2767.
[6] X.H. Zhang, P. Hu, J.C. Han, S.H. Meng, Ablation behavior of ZrB_2–SiC ultra high temperature ceramics under simulated atmospheric re-entry conditions, Compos. Sci. Technol. 68 (2008) 1718–1726.
[7] A. Rezaie, W.G. Fahrenholtz, G.E. Hilmas, Effect of hot pressing time and temperature on the microstructure and mechanical properties of ZrB_2–SiC, J. Mater. Sci. 42 (2007) 2735–2744.
[8] W.G. Fahrenholtz, G.E. Hilmas, I.G. Talmy, J.A. Zaykoshi, Refractory borides of zirconium and hafnium, J. Am. Ceram. Soc. 90 (2007) 1347–1364.
[9] S.C. Zhang, G.E. Hilmas, W.G. Fahrenholtz, Pressureless densification of zirconium diboride with boron carbide additives, J. Am. Ceram. Soc. 89 (2006) 1544–1550.
[10] W.G. Fahrenholtz, G.E. Hilmas, S.C. Zhang, S.M. Zhu, Pressureless sintering of zirconium diboride: particle size and additive effects, J. Am. Ceram. Soc. 91 (2008) 1398–1404.
[11] S.M. Zhu, W.G. Fahrenholtz, G.E. Hilmas, S.C. Zhang, Pressureless sintering of zirconium diboride using boron carbon and carbon additives, J. Am. Ceram. Soc. 90 (2007) 3660–3663.
[12] A.L. Chamberlain, W.G. Fahrenholtz, G.E. Hilmas, Pressureless sintering of zirconium diboride, J. Am. Ceram. Soc. 89 (2006) 450–456.
[13] V. Medri, C. Capiani, A. Bellosi, Properties of slip-cast and pressureless-sintered ZrB_2–SiC composites, Int. J. Appl. Ceram. Technol. 8 (2011) 351–359.
[14] V. Medri, C. Capiani, D. Gardini, Slip casting of ZrB_2–SiC composite aqueous suspensions, Adv. Eng. Mater. 12 (2010) 210–215.
[15] Z.H. Lü, D.L. Jiang, J.X. Zhang, Q.L. Lin, Aqueous tape casting of zirconium diboride, J. Am. Ceram. Soc. 92 (2009) 2212–2217.
[16] Z.H. Lü, D.L. Jiang, J.X. Zhang, Q.L. Lin, Microstructure and mechanical properties of zirconium diboride obtained by aqueous tape casting process and hot pressing, J. Am. Ceram. Soc. 93 (2010) 4153–4157.
[17] Z.H. Lü, D.L. Jiang, J.X. Zhang, Q.L. Lin, Processing and properties of ZrB_2–SiC composites obtained by aqueous tape casting and hot pressing, Ceram. Int. 37 (2011) 293–301.
[18] T.S. Huang, G.E. Hilmas, W.G. Fahrenholtz, M.C. Leu, Dispersion of zirconium diboride in an aqueous high-solids paste, Int. J. Appl. Ceram. Technol. 4 (2007) 470–479.
[19] O.O. Omatete, M.A. Janney, R.A. Strelow, Gelcasting – a new ceramic forming process, Ceram. Bull. 70 (1991) 1641–1649.

[20] A.C. Young, O.O. Omatete, M.A. Janney, P.A. Menchhofer, Gelcasting of alumina, J. Am. Ceram. Soc. 74 (1991) 612–618.
[21] D. Guo, K. Cai, L.T. Li, C.W. Nan, Z.L. Gui, Gelcasting of PZT, Ceram. Int. 29 (2003) 403–406.
[22] Z.Z. Yi, Z.P. Xie, Y. Huang, J.T. Ma, Y.B. Cheng, Study on gelcasting and properties of recrystallized silicon carbide, Ceram. Int. 28 (2002) 369–376.
[23] J.L. Yu, H.J. Wang, J. Zhang, Neural network modeling and analysis of gel casting preparation of porous Si_3N_4 ceramics, Ceram. Int. 35 (2009) 2943–2950.
[24] F.Y. Yang, X.H. Zhang, J.C. Han, S.Y. Du, Mechanical properties of short carbon fiber reinforced ZrB_2–SiC ceramic matrix composites, Mater. Lett. 62 (2008) 2925–2927.